

Crystal structure of the retinoblastoma tumor suppressor protein bound to E2F and the molecular basis of its regulation

Bing Xiao*, James Spencer*, Adrienne Clements[†], Nadeem Ali-Khan*, Sibylle Mittnacht[‡], Cristina Broceño[‡], Manfred Burghammer[§], Anastassis Perrakis[¶], Ronen Marmorstein[†], and Steven J. Gamblin*^{||}

*Division of Protein Structure, National Institute for Medical Research, Mill Hill, London NW7 1AA, United Kingdom; [†]Structural Biology Program, The Wistar Institute, and Department of Biochemistry and Biophysics, University of Pennsylvania, Philadelphia, PA 19104-4268; [‡]Institute of Cancer Research, 237 Fulham Road, London SW3 6JB, United Kingdom; [§]European Synchrotron Radiation Facility, B.P. 220, 38043 Grenoble Cedex, France; and [¶]Department of Molecular Carcinogenesis, The Netherlands Cancer Institute, 1066 CX Amsterdam, The Netherlands

Edited by Stephen C. Harrison, Children's Hospital, Boston, MA, and approved December 30, 2002 (received for review November 8, 2002)

The retinoblastoma tumor suppressor protein (pRb) regulates the cell cycle, facilitates differentiation, and restrains apoptosis. Furthermore, dysfunctional pRb is thought to be involved in the development of most human malignancies. Many of the functions of pRb are mediated by its regulation of the E2F transcription factors. To understand the structural basis for this regulation, we have determined the crystal structure of a fragment of E2F in complex with the pocket domain of the tumor suppressor protein. The pRb pocket, comprising the A and B cyclin-like domains, is the major focus of tumorigenic mutations in the protein. The fragment of E2F used in our structural studies, residues 409–426 of E2F-1, represents the core of the pRb-binding region of the transcription factor. The structure shows that E2F binds at the interface of the A and B domains of the pocket making extensive interactions with conserved residues from both. We show by solution studies that a second site, probably contained within the “marked box” region of E2F, is responsible for additional interactions with the pRb pocket but is insufficient for complex formation on its own. In addition, we show that the interaction of the core binding fragment of E2F with pRb is inhibited by phosphorylation of the tumor suppressor protein by CDK2/cyclin D/E. Finally, our data reveal that the tight binding of the human papillomavirus E7 oncoprotein to pRb prevents subsequent interactions with the marked box region of E2F but not with its core binding region.

Retinoblastoma tumor suppressor (pRb) was the first tumor suppressor protein to be cloned, and disruption of its function is now thought to be involved in the majority of human malignancies (1). pRb plays important roles in regulating the cell cycle, apoptosis, and differentiation, and all of these activities are pertinent to its role as a tumor suppressor (2). The growth-inhibitory effects of pRb are dependent on its regulation of the E2F family of transcription factors whose activity is necessary for the expression of genes involved in the G₁ to S transition of the cell cycle and DNA replication (3). pRb contains two domains that together constitute the A/B pocket (4). This region is critical for the biological activity of pRb but formation of the physiological complex of pRb with E2F, as well as its growth inhibition activity, also requires the C terminus of pRb. pRb truncated to the A/B pocket (pRb_{AB}) shows ≈10-fold weaker binding to E2F than full-length pRb (pRb_{ABC}) (5). Structures have been solved for the pocket domain of pRb in complex with a peptide derived from the papillomavirus E7 protein (4) and with a fragment of simian virus 40 (SV40) large T antigen (6).

The transcriptional activation domain of the heterodimeric E2F/DP transcription factor is contained at the C terminus of E2F. An 18-residue peptide from this domain (residues 409–426 of E2F-1) has been shown to be necessary and sufficient for specific association with pRb (7). Expression of this fragment of E2F-1, as a fusion protein with Gal4, is sufficient to recruit pRb to Gal4 promoters and subsequently repress transcription from

these sites (7). Nonetheless, several studies have suggested that there are other regions of the transcription factor that interact with pRb (8). The transcriptional repression exerted by pRb is tightly coupled to the cell cycle by the action of cyclin-dependent kinases (cdks) (9). Normal progression of the cell cycle requires that pRb is phosphorylated by G₁/S-phase specific cyclin/cdk complexes. The C-terminal domain of pRb not only contains several of the Ser/Thr residues, which are subject to cyclin/cdk modification, but is also required for normal recruitment of cyclin/cdks (10).

pRb interacts with a number of proteins containing Leu-x-Cys-x-Glu (LxCxE) motifs. These include cellular targets as well as a group of viral oncoproteins such as the papillomavirus E7 protein (11), that binds to pRb preventing complex formation with E2F. The site on pRb that binds to LxCxE-containing peptides is distinct from that which binds E2F because LxCxE-based peptides, as opposed to the full-length oncoproteins, do not inhibit E2F binding to pRb (12). Human papillomavirus (HPV), which is the etiological agent of cervical cancer in humans, encodes the E7 protein, which contains an LxCxE motif as well as a zinc-binding domain (CR3). The latter region of the protein has been shown to be necessary to enable E7 to inhibit E2F binding to pRb (13).

To better understand the regulation of the E2F transcription factor by pRb, we have determined the crystal structure of pRb_{AB} bound to E2F_(409–426). From the structure, and associated biochemical measurements, we have probed the role of interactions between pRb and regions of E2F beyond the minimal binding fragment contained in our crystal structure. We have then undertaken a further series of binding experiments to address the role of these two distinct interactions of E2F with pRb in mediating the diminution of complex formation that occurs on binding of HPV E7 protein to pRb and by phosphorylation of the tumor suppressor by cyclin/cdks.

Materials and Methods

Protein Constructs. The various protein constructs used in this study are shown schematically in Fig. 1. Rb_{AB} was expressed as a GST-fusion protein in *Escherichia coli* by using the pGEX-6P vector. The construct was engineered to contain a Precision protease site at the N terminus of Rb as well as two thrombin sites (LVPRGS) inserted at either end of the flexible A–B linker.

This paper was submitted directly (Track II) to the PNAS office.

Abbreviations: pRb, retinoblastoma tumor suppressor; HPV, human papillomavirus; ITC, isothermal titration calorimetry.

Data deposition: The coordinates and structure factors reported in this paper have been deposited in the Protein Data Bank, www.rcsb.org (PDB ID code 1o9k).

See commentary on page 2165.

^{||}To whom correspondence should be addressed. E-mail: sgambli@nimr.mrc.ac.uk.

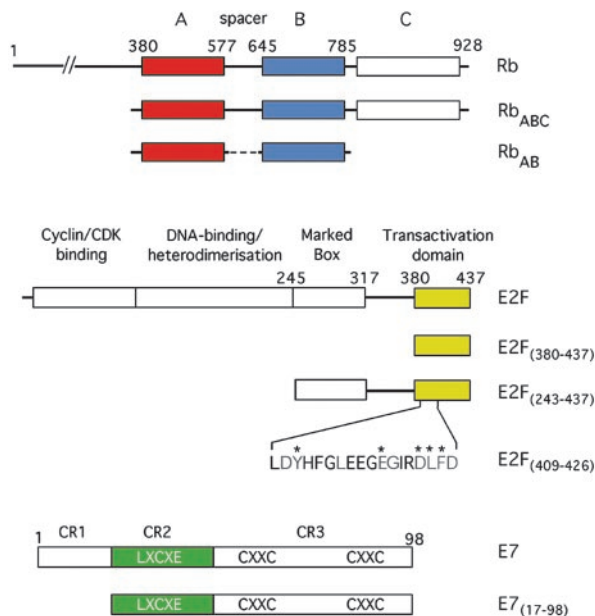


Fig. 1. Schematic drawing of functional domains and protein constructs used in this study for pRb, E2F and E7. The colors used for the constructs in this panel match those used in Fig. 2A.

Fusion protein was loaded onto a glutathione Sepharose 4B column before treatment with thrombin and PreScission protease. The resulting eluent was further purified by using a Superdex 200 gel filtration column. Rb_{ABC} was expressed in *E. coli* with a C-terminal His-tag by using pET-24. Crude lysate was first purified by using a S-Sepharose column followed by a nickel-nitrilotriacetic acid step before being run on a Superdex 200 gel filtration column. Recombinant human E2F1_(243–437) was expressed in *E. coli* by using pGEX-6P with an engineered PreScission protease site at the N terminus of E2F. Crude lysate was bound onto a glutathione Sepharose 4B column before cleavage with the protease. The resulting eluent was further purified by gel filtration on a Superdex 75 column. E2F_(409–426) and E2F_(380–437) were synthetic peptides. HPV-16 E7_(17–98) was prepared as described elsewhere (14).

Crystallography. Plate-like crystals were grown by the hanging drop vapor diffusion method at 4°C. Rb_{AB} was mixed with the E2F-1 peptide at a 1:2 molar ratio and concentrated to 15 mg/ml. Hanging drops were formed by mixing 1 μl of protein solution with an equal volume of reservoir solution containing; 0.14M Na citrate, 26% polyethylene glycol 400, 4% *n*-propanol, and 0.1M Tris at pH 7.8. Crystals were flash frozen in mother-liquor made up to 25% glycerol. Diffraction data were collected by using the microfocuss diffractometer at European Synchrotron Research Facility and processed by using the DENZO and SCALEPACK software (15). Molecular replacement calculations were carried out by using AMORE (16) with 1GUX.brk as the search model. Crystallographic statistics are presented in Table 1. Electron density, from an averaged omit map, for the E2F peptide is presented in Fig. 4, which is published as supporting information on the PNAS web site, www.pnas.org, and three views of a surface representation of pRb colored according to sequence conservation in are shown in Fig. 5A, which is published as supporting information on the PNAS web site.

Isothermal Titration Calorimetry. Binding of the various E2F constructs to Rb_{AB} and Rb_{ABC} was measured by isothermal titration calorimetry using a MicroCal Omega VP-ITC machine (Micro-

Table 1. Data and refinement statistics for the pRb/E2F_(409–426) complex

	C2
Space group	C2
Unit cell	a = 102.0 Å, b = 158.5 Å, c = 110.6 Å, β = 93.7°
Resolution range, Å	50.0–2.6
R _{sym} (%)	9.4 (45.9)
I/σ	9.1 (2.5)
Completeness, %	88.1
Final model 4 copies per au	
pRb	11,394
E2F _(409–426)	596
Water	252
R _{working} , %	22.9
R _{free} , % (5%)	28.5
rms deviation values	
Bond lengths, Å	0.010
Angles, °	1.368

Cal, Amherst, MA). The E2F constructs at a concentration between 100 and 150 μM were titrated into 12–15 μM Rb at a temperature of 22°C. Proteins were dialysed against 50 mM Tris, pH 7.6/100 mM NaCl/1 mM Tris carboxy ethyl phosphene. After subtraction of the dilution heats, calorimetric data were analyzed with the evaluation software MicroCal ORIGIN v5.0 (MicroCal Software, Northhampton, MA). For all of the titrations, the stoichiometry of ligand binding to Rb was very close to 1.0. Two ITC experiments are presented in Fig. 6, which is published as supporting information on the PNAS web site. For E2F_(243–437) and E7_(17–98) binding to Rb, the binding affinity and the heat change associated with binding were such that we could only establish that binding was tighter than 10 nM. To verify that binding of these proteins was similar for both Rb_{AB} and Rb_{ABC} we carried out competition experiments that showed approximately equal partition between the two different Rb proteins (see Fig. 7, which is published as supporting information on the PNAS web site).

Phosphorylation Assays. Phosphorylation of bacterially expressed His-6-Rb_{ABC} was conducted by using cyclin/cdk preparations from insect cells infected with recombinant baculoviruses. Kinase preparation was as described elsewhere (17). Recombinant pRb was diluted in 10 volumes of kinase buffer (50 mM Hepes-KOH, pH 7.4/10 mM MnCl₂/10 mM MgCl₂/10 mM β-glycero-phosphate/100 nM protein kinase A inhibitor/1% aprotinin/1 mM PMSF) and phosphorylated with 2 μl kinase preparation/microgram of recombinant pRb in the presence of 10 mM ATP for 30 min at 37°C. When these conditions were used, masking of the recognition by monoclonal antibody specific for underphosphorylated Ser-608 of pRb (18) to a degree greater than 90% was achieved. Reactions were stopped by adding EDTA to a final concentration of 20 mM. Mock phosphorylation was conducted by using buffer only instead of cyclin/cdk complex. Phosphorylation of individual sites was routinely monitored by using phosphorylation site-specific pRb antibodies described in Rubin *et al.* (19) and these results are given in Fig. 8, which is published as supporting information on the PNAS web site. pRb preparations were supplemented with glycerol to a final concentration of 50% and stored at –20°C. Four micrograms of Rb_{ABC} was adsorbed to 30 μl of Talon beads, washed extensively in binding buffer (125 mM NaCl/25 mM Hepes, pH 7.0/0.1% Triton X-100/3 μg/μl BSA/0.2 mM PMSF/1% vol/vol aprotinin/10 mM NaF/10 mM β-glycerophosphate) and incubated with a molar excess of ligand [2-fold for E2F_(243–437) and 48-fold for the weaker binding E2F_(380–437)] for 4 h. Binding reactions were washed twice with

0.5 ml of binding buffer, eluted with 10 mM EDTA, then boiled into sample buffer and, after separation on 10–20% Tris-tricine gradient gels, transferred onto Immobilon membrane and probed with antiserum specific for the C terminus of E2F (Santa Cruz Biotechnology, C20) or Rb (Santa Cruz Biotechnology, C15), both of which are affinity purified.

Results and Discussion

Structure of the pRb/E2F Complex. Crystals of the pRb/E2F_(409–426) complex grew in a plate-like habit with typical dimensions $200 \times 200 \times 10 \mu\text{m}^3$. Repeated attempts at data collection from flash-cooled crystals using synchrotron x-ray sources were thwarted by very high crystal mosaicity and the resulting data could not be adequately scaled. Using the same crystals, a data set was collected by using the microfocus diffractometer on station ID13 at ESRF (20), currently the only such device installed at a synchrotron source, utilizing a $10 \times 10 \mu\text{m}^2$ aperture. The diffraction images from the microdiffractometer displayed much lower mosaicity and produced a good quality data set on data scaling and reduction. The structure was solved by molecular replacement and produced initial electron density maps in which the E2F peptide could be readily located. The packing of the A and B domains generates a waist-like interface groove into which E2F_(409–426) binds in a largely extended manner (Fig. 2A). The peptide makes contacts with residues from helices α_4 , α_5 , α_6 , α_8 , and α_9 of domain A, and with α_{11} from domain B of pRb. Formation of the complex buries 2,280 \AA^2 of surface area, 1,500 \AA^2 of which are hydrophobic. The two end regions of the E2F peptide make extensive contacts with pRb, whereas interactions made by the middle section of E2F (residues 416 to 420) are relatively sparse (Fig. 2B). Overall, a high proportion of the hydrogen bond interactions between the two molecules involve the side chains of conserved pRb residues interacting with the main chain of E2F (see Fig. 6A).

Within the E2F_(409–426) construct there are nine residues that are conserved across E2F's from all animal species (Fig. 2B). Amino acid substitutions at five of these positions have been shown to lead to loss of binding to pRb but retention of E2F's transactivation potential (21). The following description focuses on the structural role of these five residues. Tyr(411)-E2F appears to play an important role in peptide binding because its phenolic ring occupies a hydrophobic pocket created by Ile(536)-pRb, Ile(532)-pRb, Ile(547)-pRb, and Phe(413)-E2F, whereas its hydroxyl group makes a hydrogen bond to the invariant Glu(554)-pRb. Toward the C-terminal part of the E2F peptide, Leu(424)-E2F and Phe(425)-E2F make several hydrophobic interactions, two of which involve conserved residues. Leu(424)-E2F makes contacts with the aliphatic portion of the side chain of Lys(530)-pRb and also packs against Leu(415)-E2F and Phe(425)-E2F. In addition, Phe(425)-E2F itself packs against Phe(482)-pRb. Unlike the residues of E2F just discussed, the side-chains of Glu(419)-E2F and Asp(423)-E2F do not point into the groove formed between the A and B domains of pRb, but instead point away from it. Glu(419)-E2F hydrogen bonds through a water molecule with the main-chain carbonyl of Thr(645)-pRb; Asp(423)-E2F forms a salt bridge with Arg(467)-pRb located on α_4 .

Because there are four copies of the pRb/E2F complex in the asymmetric unit of our crystal form, it is possible both to compare these four crystallographically independent copies of the pRb/E2F complex and to compare them with the crystal structure of pRb/E7 without bound E2F (4). The first six residues at the N terminus, the α_3 - α_4 and α_6 - α_7 loops adopt different conformations between the four copies in our asymmetric unit, whereas the variations across the rest of the structure between the four molecules is not significant. Comparison of the pRb structure in the presence and absence of bound E2F shows that there is essentially no change in the relative orientation of

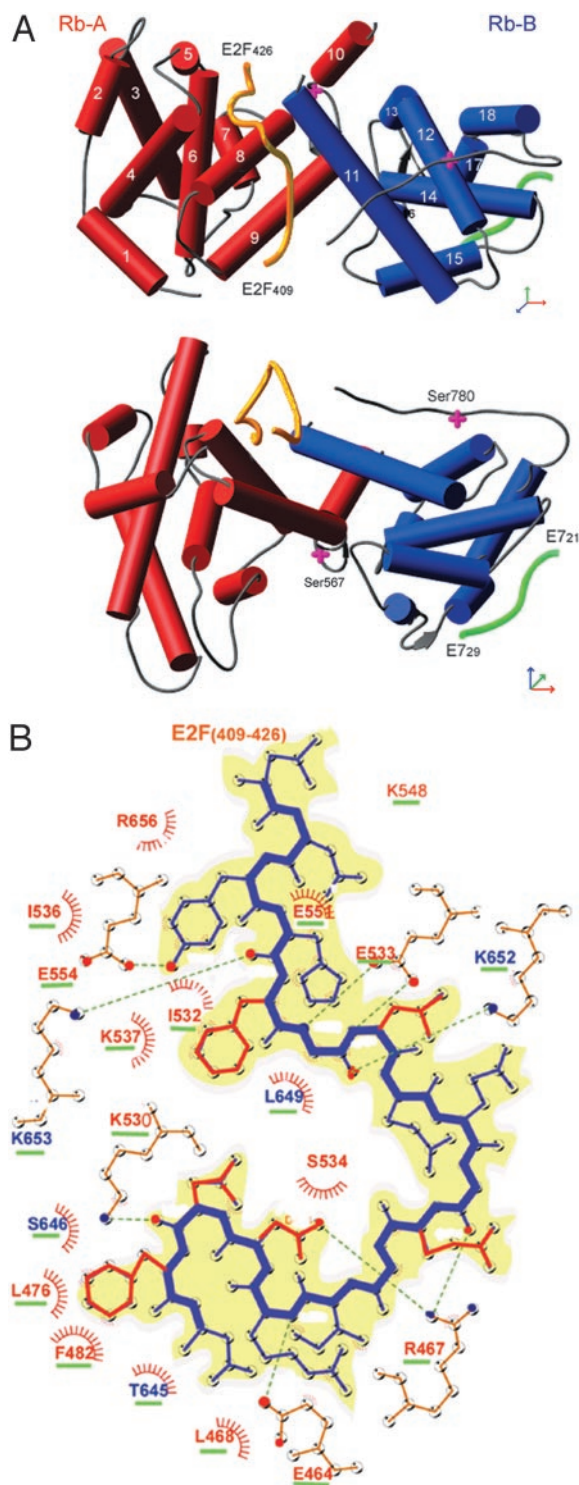


Fig. 2. Structure of pRb/E2F. (A) The structure of Rb_{AB}/E2F_(409–426), shown in two orthogonal views in Ribbons representation (27). The helices of the A domain are shown as red cylinders and those of the B domain are shown as blue cylinders. The main-chain trace of E2F and E7 (from 1GUX) are shown as yellow and green worms, respectively. (B Upper) Schematic representation of the C terminus of E2F with residues 409–426 shown in single letter code. Those residues conserved across the E2F family are shown in red, whereas residues whose mutation alters binding to pRb are starred. (Lower) Interactions between E2F_(409–426) and Rb_{AB} are shown schematically (drawn with LIGPLOT). Hydrogen-bond interactions are shown as broken green lines, whereas hydrophobic contacts are indicated by red spoked arcs. Residues from domain A of pRb are colored red and residues from domain B are colored blue; conserved residues are underlined in green. The side chains of conserved E2F residues are colored red as in the Upper.

Table 2. ITC measurements

Binding constants, μM	Rb _{AB}	Rb _{AB} /E7	Rb _{ABC}	Rb _{ABC} /E7
E2F (409–426)	0.34 ± 0.02	0.35 ± 0.02	0.3 ± 0.03	0.36 ± 0.10
E2F (380–437)	0.16 ± 0.01	0.18 ± 0.06	0.1 ± 0.01	0.18 ± 0.07
E2F (243–437)	<0.01	0.12 ± 0.03	<0.01	0.36 ± 0.13
E7 (17–98)	<0.01	–	<0.01	–

Summary of dissociation constants obtained by ITC measurements. The quoted errors are those produced by fitting the data to a two-state model. For the interaction of E2F_(243–437) and E7_(17–98) to Rb_{AB} and Rb_{ABC} the affinities are too high to measure reliably and we have therefore quoted the upper limits of the dissociation constants.

the two lobes of the A/B pocket on E2F binding nor any widespread changes in the structures of the individual domains. This comparison does reveal that the end of $\alpha 4$ and the connecting loop to $\alpha 5$ becomes ordered in the pRb/E2F complex as two conserved residues (Glu-464-pRb and Arg-467-pRb located toward the end of $\alpha 4$ in our structure) interact with the E2F peptide (shown in Fig. 5B).

Additional Determinants of pRb/E2F Interaction. It is clear from a number of studies that, although E2F_(409–426) expressed as a Gal4 fusion protein is sufficient to recruit pRb and repress transcription, there are additional interactions made by the physiologically relevant E2F/DP heterodimer with pRb. Similarly, although the pocket domain is highly conserved, the most frequent site of deleterious mutation, and capable of transcriptional repression, it is not sufficient for the physiological function of pRb. In particular, the C terminus of pRb is necessary for mediating growth arrest and recruitment of certain cyclin/cdk complexes as well as containing several of the residues whose phosphorylation leads to deactivation of pRb function. Therefore, we have made a series of constructs of the two proteins (see Fig. 1) and carried out binding measurements by isothermal titration calorimetry (ITC).

A summary of the affinity constants obtained for both pRb_{AB} (the pRb pocket domain) and pRb_{ABC} (the pocket domain and C terminus domain of pRb) interacting with three constructs of E2F are given in Table 2. The two shorter E2F constructs bind to either pRb_{AB} or pRb_{ABC} with similar affinities. However, E2F_(243–437) binds at least 16-fold stronger than either of the two shorter E2F fragments to both pRb_{AB} and Rb_{ABC}. Our ITC data are consistent with an earlier report (8) that suggested that there is an additional interaction of pRb with the marked box region of E2F (residues 245–317). Taken together, these data demonstrate that the majority of the free energy of interaction between pRb and E2F is contributed by the 18-residue segment E2F_(409–426) used in our structure analysis. However, there is an additional stabilising interaction between the marked box region of E2F and pRb, that contributes $\approx 2 \text{ kcal}\cdot\text{mol}^{-1}$ to the overall free energy of binding, but is not sufficient on its own for complex formation (7).

Regulation of pRb Binding to E2F by Phosphorylation. It is thought that the C terminus of pRb plays an important role in phosphorylation-dependent deactivation of the tumor suppressor protein. To better understand the molecular basis of this mechanism we have looked at the effects of phosphorylation on pRb_{ABC} binding to two different E2F constructs. Specifically, we wanted to determine whether phosphorylation of pRb prevents it from binding the minimal pRb-binding fragment of E2F. A series of pull-down experiments using E2F_(380–437) and E2F_(243–437) were carried out. The experiment was repeated three times and in all cases gave the same result, one example of which is shown in Fig. 3. The results show that prior phosphorylation of pRb by either cyclin

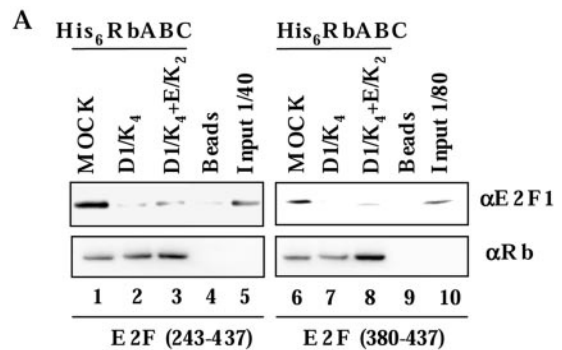


Fig. 3. Western blot showing the effect of prephosphorylation of pRb on subsequent binding of two different E2F constructs: E2F_(243–437) (lanes 1–5) and E2F_(380–437) (lanes 6–10). The His-6-pRb was treated with cyclinD1/CDK4 (D1/K4), cyclinD1/CDK4 + cyclinE/CDK2 (D1/K4+E/K2), or buffer alone (MOCK). The His-6-pRb was used in pull-down experiments using Talon beads, and the resulting gels were probed with antiserum specific for the C terminus of E2F or pRb. The gel shows that either phosphorylation treatment of pRb reduces the level of E2F binding to that of the background level obtained by using beads without pRb.

D/cdk or by cyclin (D + E)/cdk, reduces the level of E2F binding to that of background and that the result is the same for the two E2F constructs tested. For these experiments we used E2F_(380–437) in place of E2F_(409–426) because of the available antibodies. In these experiments the amount of binding of E2F_(380–437) to unphosphorylated pRb is less than that seen for E2F_(243–437). As discussed above, this arises because the shorter construct binds at least 16-fold weaker than the longer one. Because a lower proportion of E2F_(380–437) binds to unphosphorylated pRb than does E2F_(243–437), the difference in the amount of E2F_(380–437) bound to phosphorylated pRb, relative to unphosphorylated pRb, is also less than that observed for E2F_(243–437). Nonetheless, it is apparent that phosphorylation of pRb reduces the binding of E2F_(380–437) and E2F_(243–437) to background levels. Because the crystallised E2F_(409–426) fragment binds with similar affinity as E2F_(380–437) our binding studies suggest that the interactions described in our crystal structure are indeed the target of phospho-regulation.

Harbor *et al.* (22) have shown that phosphorylation of Ser-567-pRb *in vitro* (see Fig. 2A) by cyclinE/cdk2, leads to disruption of the A/B interface of the tumor suppressor and thus to release of bound E2F. Indeed, the side chain of Ser-567-pRb is oriented into a cavity on the molecules surface that is lined with hydrophobic residues and phosphorylation of this residue would seem likely to lead to substantial destabilization of the structure. Our crystal structure shows that the binding of E2F to pRb involves many interactions with both the A and B domains and is also dependent on the integrity of the interface between them. Our crystal structure therefore provides a molecular rationale of how phosphorylation at Ser-567 disrupts the binding of E2F_(409–426). Harbor *et al.* (22) also provide evidence that phosphorylation of pRb promotes various intramolecular interactions between the A/B pocket and phosphorylated segments of the protein that alters the binding properties of the tumor suppressor. Our crystal structure reveals that eight basic residues from the A/B domain interface of pRb participate in binding to the highly acidic E2F peptide (residues 409–426) and would evidently be well suited for interaction with either phosphoserine or phosphothreonine residues. It seems possible that phospho-regulation of pRb/E2F may occur by at least two distinct mechanisms; one involving disruption of the pocket structure, the other by promoting an intramolecular competition for the E2F binding site. Moreover, these distinct mechanisms

may pertain to different regulatory scenarios; in one case phosphorylation of free pRb prevents its subsequent binding to E2F, a second case is where phosphorylation leads to disruption of an existing pRb/E2F complex. Clearly an understanding of the physiologically relevant regulatory mechanisms of pRb will require more extensive biochemical and cell biological studies.

Structural Basis of HPV E7 Action. Although endogenous factors diminish the binding affinity of pRb for E2F by phosphorylation, certain oncogenic viruses produce specific proteins for this purpose. Given the importance of HPV in the development of cervical cancer (11, 24) we were interested to examine the mechanism by which its E7 protein targets the pRb/E2F complex. We and others have demonstrated that binding of E2F_(409–426) and an 8-residue peptide based on the LxCxE motif of E7 to pRb are independent events (4). The structure presented here, taken with that of the pRb/E7-peptide complex (4), shows that these two binding sites are non-overlapping and are indeed more than 30 Å apart on the surface of pRb (Fig. 2A). How then does full-length HPV E7 prevent E2F from binding to pRb? It has previously been shown that a construct encompassing residues 17–98 of HPV E7, which includes the LxCxE motif as well as the CR3 domain, is sufficient and necessary to inhibit pRb binding to E2F (13). Therefore, we first determined the binding affinity of E7_(17–98) for pRb_{AB} and pRb_{ABC}. These data, summarized in Table 2, show that both pRb constructs bind tightly (<10 nM) to E7_(17–98). Competition experiments (data not shown) confirmed earlier work suggesting that E7 binds tighter to Rb_{ABC} than Rb_{AB} (25). Importantly, however, our results demonstrate that E7_(17–98) binds at least 15-fold tighter than E7 peptides based on the LxCxE motif to both pRb constructs, and thus demonstrate that the CR3 domain of E7 makes interactions with the A/B pocket, as well as with the C terminus of pRb. Next, we made stoichiometric complexes of pRb/E7_(17–98) and carried out binding titrations with E2F_(409–426), E2F_(380–437) and E2F_(243–437). The data in Table 2 show that preforming a complex between E7 and pRb (either pRb_{AB} or pRb_{ABC}) has little or no effect on the subsequent binding of E2F_(409–426) or E2F_(380–437) but that it reduces the apparent binding affinity of E2F_(243–437) by at least 12-fold. These data indicate that E7_(17–98) competes with E2F_(243–437) for binding to pRb but that it binds independently of either of the two shorter constructs of E2F. We have confirmed these observations using competition experiments that are presented in Fig. 7. Taken with earlier data (13), our results suggest that the CR3 domain of E7 interacts with the A/B pocket of pRb such that it interferes with subsequent binding of the marked box of E2F. Moreover, the fact that the binding constant for E2F_(243–436) interacting with pRb/E7 is reduced to close to that of E2F_(409–426) binding to pRb alone further suggests that the two pRb-binding sites on E2F are not part of a rigid complex. Instead, it appears that the marked box region and transactivation domain of E2F are joined by a flexible linker, and though the two sites are tethered together, they bind independently to pRb. There are at least two mechanisms by which the CR3 domain of E7 may interfere with the binding of the marked box region of E2F with the AB pocket of pRb. First, that there is, at least partial, overlap between the binding sites for the CR3 domain of E7 and the marked box region of E2F on the surface of pRb. Second, that the binding of E7 to pRb induces a conformational change in the tumor suppressor protein such that it no longer recognizes the marked box region of E2F. Discrim-

ination between these two models will require further detailed biochemical investigations and probably the determination of the crystal structure of a pRb/E7 complex. Nevertheless, the overall effect of E7 binding to pRb is to negate the binding contribution made by the marked box region of E2F and hence reduce the overall binding affinity of pRb for the transcription factor by approximately one order of magnitude. It is feasible that this change in affinity of pRb for E2F enables sufficient E2F driven transcription for the virus to be able to replicate without generating so much free E2F activity that apoptosis is induced.

Although inactivation of the pRb pathway is thought to be widely involved in cellular transformation, there are examples of tumors where overexpression of functional pRb appears to be detrimental to successful clinical treatment. Adenocarcinoma of the pancreas is the fifth most common cause of cancer-related death in the Western world. It is particularly resistant to currently available forms of chemotherapy and radiation therapy. It is thought that this malignancy is able to evade apoptosis induced by treatment with chemotherapeutic drugs because of overexpression of pRb (26). It seems plausible that the inhibitory effect of pRb overexpression on apoptosis may be mediated by E2F. By blocking transcriptional activation by E2F, overexpression of pRb appears to render pancreatic cancer cells insensitive to chemotherapy. Given our description of the molecular interactions between E2F and the A/B interface of pRb it should be possible to develop compounds that bind to pRb and inhibit complex formation. Such a compound, administered in parallel with conventional chemotherapy, may offer a means of treatment for pancreatic cancer and perhaps related diseases.

In this work we have presented the structure of the A/B pocket of pRb in complex with E2F_(409–426). This region of E2F represents the core binding region of the transcription factor for pRb. The structure provides a detailed molecular description of how this region of E2F binds at the interface between the A and B domains. With this data it should be possible to design site-specific mutants of pRb that no longer bind E2F, but whose other properties are unaltered. Such altered pRb should be a valuable tool for cell biology experiments aimed at probing the function of pRb/E2F interactions. We show that there is an additional interaction made between E2F and pRb. This likely arises from the marked box region of E2F and enhances the overall affinity of the interaction by ≈15-fold. We provide evidence that it is this second, comparatively weak, interaction that is targeted by the papillomavirus E7 protein. Clearly this idea needs to be further tested but has important implications for how HPV manipulates the cell cycle machinery of host organisms by relatively subtle changes in the affinity of interacting proteins. In contrast, our data suggest that the phosphorylation of pRb leads to loss of binding to the core pRb-binding region of E2F and that this represents a more substantial switch in the affinity of pRb for E2F.

We acknowledge D. Emery for protein expression constructs and C. Jing and S. Price for assistance with protein purification. We are grateful to A. Lane and K. Rittinger for critical reading of the manuscript, S. Smerdon for helpful discussions, and K. Lin and W. Taylor for assistance with sequence alignments. We thank the staff of Synchrotron Radiation Source Daresbury and European Synchrotron Radiation Facility Grenoble for synchrotron access, and we acknowledge financial support from a European Molecular Biology Laboratory European Union Access to Research Infrastructures grant. A.C. was funded by a grant from the Department of Defense U.S. Army Breast Cancer Program, and work in R.M.'s laboratory was supported by grants from American Cancer Society and National Institutes of Health.

- Weinberg, R. A. (1995) *Cell* **81**, 323–330.
- Hickman, E. S., Moroni, M. C. & Helin, K. (2002) *Curr. Opin. Genet. Dev.* **12**, 60–66.
- Goodrich, D. W., Wang, N. P., Qian, Y. W., Lee, E. Y. & Lee, W. H. (1991) *Cell* **67**, 293–302.
- Lee, J. O., Russo, A. A. & Pavletich, N. P. (1998) *Nature* **391**, 859–865.

- Qin, X. Q., Chittenden, T., Livingston, D. M. & Kaelin, W. G. (1992) *Genes Dev.* **6**, 953–964.
- Kim, H. Y., Ahn, B. Y. & Cho, Y. (2001) *EMBO J.* **20**, 295–304.
- Helin, K., Lees, J. A., Vidal, M., Dyson, N., Harlow, E. & Fattaey, A. (1992) *Cell* **70**, 337–350.

8. O'Connor, R. J. & Hearing, P. (1994) *J. Virol.* **68**, 6848–6862.
9. Adams, P. D. (2001) *Biochim. Biophys. Acta* **1471**, M123–M133.
10. Adams, P. D., Li, X., Sellers, W. R., Baker, K. B., Leng, X., Harper, J. W., Taya, Y. & Kaelin, W. G., Jr. (1999) *Mol. Cell. Biol.* **19**, 1068–1080.
11. Munger, K., Werness, B. A., Dyson, N., Phelps, W. C., Harlow, E. & Howley, P. M. (1989) *EMBO J.* **8**, 4099–4105.
12. Wu, E. W., Clemens, K. E., Heck, D. V. & Munger, K. (1993) *J. Virol.* **67**, 2402–2407.
13. Huang, P. S., Patrick, D. R., Edwards, G., Goodhart, P. J., Huber, H. E., Miles, L., Garsky, V. M., Oliff, A. & Heimbroom, D. C. (1993) *Mol. Cell. Biol.* **13**, 953–960.
14. Clements, A. J., K. Mazzei, J. M. Ricciardi, R. P. Marmorstein R. (2000) *Biochemistry* **39**, 16033–16045.
15. Otwinowski, Z. & Minor, W. (1993) in *Data Collection and Processing*, eds. Sawyer, L., Isaacs, N. & Bailey, S. (Science and Engineering Research Council Daresbury Laboratory, Cheshire, Warrington, U.K.), pp. 556–562.
16. Collaborative Computational Project No. 4 (1994) *Acta Crystallogr. D* **50**, 760–763.
17. Zarkowska, T. & Mittnacht, S. (1997) *J. Biol. Chem.* **272**, 12738–12746.
18. Zarkowska, T., U, S., Harlow, E. & Mittnacht, S. (1997) *Oncogene* **14**, 249–254.
19. Rubin, E., Mittnacht, S., Villa-Moruzzi, E. & Ludlow, J. W. (2001) *Oncogene* **20**, 3776–3785.
20. Perrakis, A., Cipriani, F., Castaga, J., Claustre, L., Burghammer, M., Riek, C. & Cusack, S. (1999) *Acta Crystallogr. D* **55**, 1765–1770.
21. Shan, B., Durfee, T. & Lee, W. H. (1996) *Proc. Natl. Acad. Sci. USA* **93**, 679–684.
22. Harbour, J. W., Luo, R. X., Dei Santi, A., Postigo, A. A. & Dean, D. C. (1999) *Cell* **98**, 859–869.
23. Knudsen, E. S. & Wang, J. Y. (1997) *Mol. Cell. Biol.* **17**, 5771–5783.
24. Edmonds, C. & Vousden, K. H. (1989) *J. Virol.* **63**, 2650–2656.
25. Patrick, D. R., Oliff, A. & Heimbroom, D. C. (1994) *J. Biol. Chem.* **269**, 6842–6850.
26. Plath, T., Peters, M., Detjen, K., Welzel, M., von Marschall, Z., Radke, C., Wiedenmann, B. & Rosewicz, S. (2002) *J. Natl. Cancer Inst.* **94**, 129–142.
27. Carson, M. (1991) *J. Appl. Crystallogr.* **24**, 958–961.